*Geopersia* ***5*** *(2), 2015, PP. 161-175*

# Use of nanoscale zero-valent iron to improve the shear strength parameters of gas oil contaminated clay

**Sayed Alireza Nasehi[1], Ali Uromeihy[1]*, Ali Morsali[2], Mohammad Reza Nikudel[1]**
[1] *Engineering Geology Division, Department of Geology, Faculty of Basic Sciences, Tarbiat Modares University, Iran.*
[2] *Department of Chemistry, Faculty of Basic Sciences, Tarbiat Modares University, Iran.*
**Corresponding author, e-mail: uromeiea@modares.ac.ir*

(*received: 11/07/2015 ; accepted: 25/11/2015*)

## Abstract

In recent years, the nanoscale zero-valent iron (NZVI) particles have been used successfully for the degradation of hydrocarbon compounds and remediation of other pollutants. Nevertheless, as far as we know, there is no specific study on the improvement of the geotechnical properties of contaminated soils with hydrocarbon compounds by NZVI. This study used NZVI particles to remove gas oil in a clayey soil and determined the effects of NZVI on Atterberg limits, compaction properties, and shear strength parameters of the soil. In order to determine the optimal reaction time and NZVI dosage, the total organic carbon (TOC) of a contaminated soil with 9% of gas oil was measured. The experimental data showed that the optimum reaction time and NZVI dosage were 24 days and 5%, respectively. Then, the contaminated samples were prepared by mixing the soil with gas oil in the amount of 0, 3, 6, and 9% by dry weight. The results showed a decrease in the friction angle (φ) and an increase in the cohesion (C). Maximum dry density and optimum moisture content of the soil decreased due to the contamination. In addition, an increase in liquid limit (LL) and plastic limit (PL) were observed. Finally, all contaminated specimens were mixed with 5% of NZVI. After 24 days, an increase was seen in the friction angle, cohesion, maximum dry density, and optimum water content. LL and PL of the soil decreased after the treatment

**Keywords:** *Clay, Contamination, Gas Oil, Nanoscale Zero-Valent Iron, NZVI, Shear Strength Parameters.*

## Introduction

Particles in the nano-sized range have been present on earth for millions of years and used by humankind for thousands of years. For example, soot is a product of the incomplete combustion of fossil fuels and vegetation; it has a particle size in the nanometer-micrometer range and, therefore, falls partially within the “nanoparticle” domain. Recently, however, nanoparticles have attracted a lot of attention because of our increasing ability to synthesize and manipulate such materials. Today, nanoscale materials are used in a variety of different areas such as electronic, biomedical, pharmaceutical, cosmetic, energy, environmental, catalytic, and material applications (Nowack and Bucheli, 2007).

There are two types of nanoparticles: natural and engineered. According to Bhatt and Tripathi (2011), natural nanoparticles divide into inorganic (silicates, oxides, hydroxides, carbonates, phosphates, and metal sulfides) and organic (macromolecules, bio-colloids, and cellular debris). Engineered nanoparticles divide into unintentional (wear and corrosion, as well as waste and combustion, products) and intentional (carbonaceous nanoparticles, metal oxides, semiconductor materials, zero-valent metals, and nanopolymers). Among the engineered nanoparticles, zero-valent metals are usually prepared by reduction of metals. For example, zero-valent iron is made through the reduction of ferric ($Fe^{3+}$) or ferrous ($Fe^{2+}$) salts with a sodium borohydride (Li *et al*., 2006).

Most environmental applications of nanotechnology and nanoparticles fall into three categories: (1) environmentally-benign and/or sustainable products (e.g. green chemistry or pollution prevention), (2) remediation of materials contaminated with hazardous substances, and (3) sensors for environmental agents (Tratnyek and Johnson, 2006).

Nanoscale zero-valent metals, especially nanoscale zero-valent iron (NZVI), have many applications for the remediation of materials contaminated by hazardous substances. NZVI has found usage in the remediation of water, soils, and sediments for removing contaminants. According to Zhang (2003), common environmental contaminants that can be transformed by NZVI are as follows: chlorinated methanes (e.g. chloroform), chlorinated benzenes (e.g. chlorobenzene), pesticides (e.g. DDT), heavy metal ions (e.g. nickel and mercury), inorganic anions (e.g. arsenic and nitrate), polychlorinated hydrocarbons (e.g. polychlorinated biphenyls), and chlorinated ethenes (e.g. tetrachloroethene). Extensive studies have been carried out on the dehalogenated organic pollutants in soils and groundwater by NZVI (Varanasi *et al*., 2007; Zhang *et al*., 2012; Wang and Zhang, 1997; Lien and Zhang, 1999; Matheson and Tratnyek, 1994; Song and Carraway, 2005; Gillham and O’Hannesin, 1994). The chemical principles underlying the transformation of halogenated hydrocarbons have been particularly well documented (Li *et al*., 2006). Metallic iron ($Fe^{\circ}$) serves effectively as an electron donor:

$$Fe^{\circ} \longrightarrow Fe^{2+} + 2e^{-} \qquad (1)$$

Chlorinated hydrocarbons, on the other hand, accept the electrons and undergo reductive dechlorination:

$$RCl + H^{+} + 2e^{-} \longrightarrow RH + Cl^{-} \qquad (2)$$

From a thermodynamic prospective, the coupling of the reactions (1) and (2) is often energetically highly favorable:

$$RCl + Fe^{\circ} + H^{+} \longrightarrow RH + Fe^{2+} + Cl^{-} \qquad (3)$$

For example, tetrachloroethene ($C_2Cl_4$) can be completely reduced to ethane gas by NZVI in accordance with the following overall equation:

$$C_2Cl_4 + 5Fe + 6H^{+} \longrightarrow C_2H_6 + 5Fe^{2+} + 4Cl^{-} \qquad (4)$$

In addition to the dehalogenation of hydrocarbons by using NZVI, the degradation of non-halogenated hydrocarbon compounds has been reported by Chang *et al*. (2005). They used micro and nanoscale zero-valent iron to remove a polycyclic aromatic hydrocarbon, pyrene, in soil. The results showed that both the micro and nanoscale zero-valent irons were capable of removing the target compound in soil, but higher removal efficiencies were achieved by nanoscale zero-valent iron because of the massive specific surface area (SSA).

Nevertheless, as far as we know, there is no specific study on the improvement of geotechnical properties of contaminated soils with hydrocarbon compounds, such as gas oil by NZVI. Therefore, the objective of this research was to perform laboratory testing program in order to determine the effects of NZVI on the geotechnical characteristics of a clayey soil contaminated by gas oil. These properties included Atterberg limits (LL and PL), compaction characteristics, and the shear strength parameters (C and φ) of the soil.

## Materials and Methods

The soil used for the study was clay collected from the area of Neyriz, east of Fars province, in the south of Iran. Figure 1 shows the particle size distribution of the studied soil according to ASTM D422 (1999). It is classified as CL (low plasticity clay) according to the Unified Soil Classification System. Specific gravity and liquid and plastic limits were determined based on ASTM D854 (1999) and ASTM D4318 (1999), respectively. The standard Proctor compaction tests were performed on the soil samples based on ASTM D698 (1999). The specific surface area (SSA) of the soil was measured by Ethylene Glycol Monoethyl Ether (EGME) method (Carter *et al*., 1965). Tables 1 and 2 show the summary of the soil’s basic properties and the result of X-ray diffraction (XRD) analysis used to determine the mineralogy of the soil, respectively. Table 3 includes the properties of the gas oil used in this study. NZVI was obtained from US Research Nanomaterials, Inc. The distribution of particle size (Fig. 2) and zeta potential (ζ) of NZVI were measured by Horiba LB-550 and Horiba SZ-100 instruments.

Table 1. The soil properties

| Soil | LL (%) | PL (%) | Gs | $\rho_{dmax}$ (g/cm$^3$) | $w_{opt}$ (%) | Percent finer than 2μm | Specific surface area,(m$^2$/g) | Total Carbon (%) | pH |
|---|---|---|---|---|---|---|---|---|---|
| CL | 47.87 | 23.45 | 2.55 | 1.61 | 21.2 | 18.03 | 32.16 | 0.86 | 6.69 |

Table 2. Mineralogy of the soil (XRD results)

| Soil type | Minerals |
|---|---|
| CL | Calcite, quartz, albite, muscovite, clinochlore |

Table 3. The gas oil properties (from the supplier, NIORDC, Iran)

| **Density at 25°C ($g/cm^3$)** | **Ignition temperature (°C)** | **Self-ignition temperature (°C)** | **Boiling point (°C)** | **Dynamic Viscosity at 20°C (cP)** |
|---|---|---|---|---|
| 0.80 - 0.84 | 56 | 257 | 150 - 390 | 1.7 - 2 |

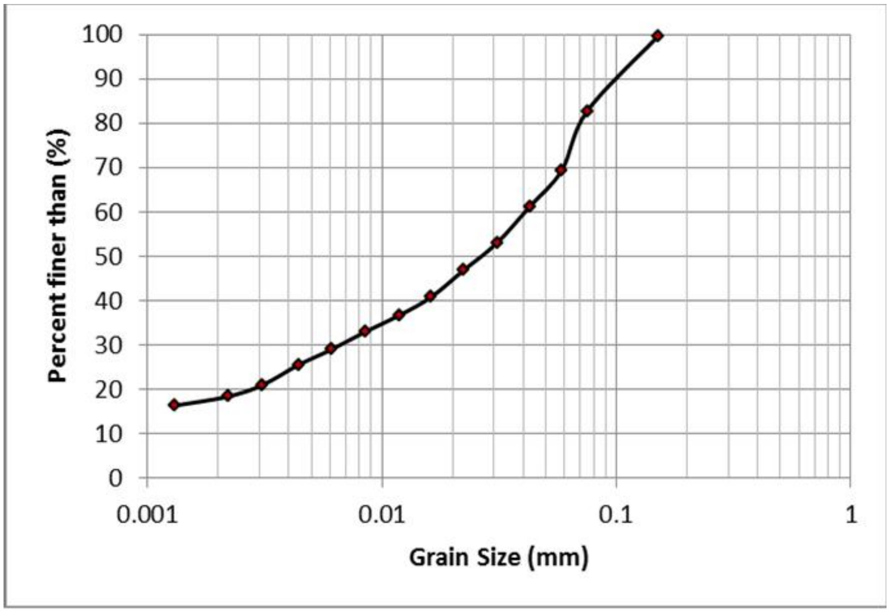

Figure 1. Particle size distribution curve of the soil

The purity of NZVI was determined by X-ray fluorescence (XRF) analysis (Table 4). Table 5 shows the properties of the NZVI used in this study. The SSA of NZVI was measured by nitrogen gas-adsorption BET method (Brunauer *et al.*, 1938). The amount of TOC of the samples was determined by CHN analyzer (CHN Thermo Finnigan Flash EA 1112) after 3, 10, 17, 24, 31, and 38 days. The initial total carbon (TC) of the soil (Table 1) was subtracted from the TOC amount. At the mentioned time, the pH of the specimens was measured according to the ASTM D4972 (1999). Distilled water, equal to the optimum moisture content, was added to all samples. The mineralogy of the clay and non-clay minerals of the soil, after mixing with NZVI, was identified by XRD test. Semi-quantitative estimation of clay minerals was based on peak areas and on peak heights for non-clay minerals, as proposed by Pierce and Siegel (1969). Table 6 shows the name of the samples prepared.

## Sample preparation

In this research, the laboratory testing program was accomplished in two stages. In the first stage, after particle size classification, samples were dried by an oven at 105°C for 24h. Then, the gas oil was sprayed on the samples and mixed manually with soils in the amount of 0, 3, 6 and 9% by weight of the dry soil specimens. The mixture was put into closed containers in room temperature for 1 month to reach equilibrium. For a direct shear test, the standard Proctor compaction test was done to find the density and the optimum moisture content of the samples at different percentages of contamination. Then, the samples for direct shear test were remolded in the mold with static compaction at the determined maximum dry density and optimum moisture content. The test was carried out according to ASTM D3080 (1999).

In the second stage, to determine the effect of NZVI on the amount of gas oil at the mentioned time, 1, 3, 5, and 7% of NZVI were added to samples of the soil contaminated with 9% of the contaminant. After mixing and homogenization, the specimens were put into closed vials in room temperature. All of the geotechnical tests that were done in the first stage were performed on the samples mixed with the optimum amount of NZVI in the second stage.

Table 4. XRF analysis of NZVI

| **Chemical component** | $Al_2O_3$ | $SiO_2$ | $P_2O_5$ | $SO_3$ | $Fe_2O_3$ | MnO | $TiO_2$ |
|---|---|---|---|---|---|---|---|
| **Percentage** | 0.154 | 0.261 | 0.031 | 0.052 | 99.026 | 0.326 | 0.15 |

Table 5. The NZVI properties

| **Color** | **Purity (%)** | **Shape** | **Specific gravity** | **Specific surface area, ($m^2/g$)** | **ζ potential (mV)** |
|---|---|---|---|---|---|
| Black | 99.03 | Spherical | 7.85 | 48.54 | + 17.4 |

Table 6. The names of soil samples

| **Sample name** | | **Gas oil Content, (%)** |
|---|---|---|
| CL | CL + NZVI* | |
| CL0 | CL0 + NZVI | 0 |
| CL3 | CL3 + NZVI | 3 |
| CL6 | CL6 + NZVI | 6 |
| CL9 | CL9 + NZVI | 9 |

* 5% of NZVI

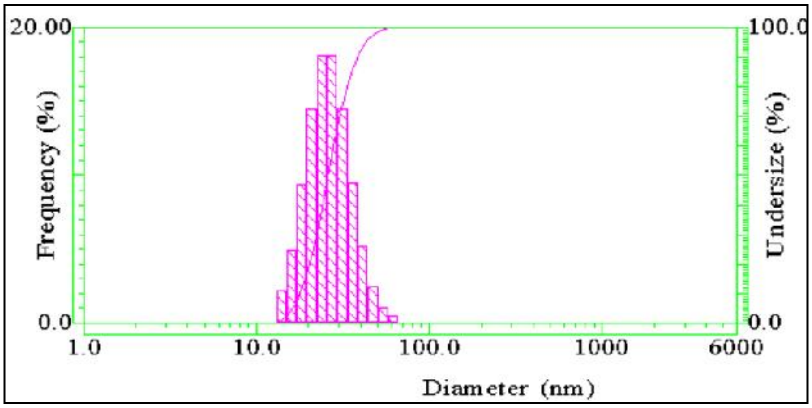

Figure. 2. Particle size distribution chart of the NZVI

## Discussion

### *Mineralogical analysis*

The results of XRD on the clean and untreated soil sample indicated that the clinochlore (a member of chlorite group) was the principal clay mineral of the soil (Fig. 3). Other non-clay minerals were also detected in the bulk sample, including calcite, quartz, albite, muscovite, and dolomite. As can be seen in Figures 4 and 5, the XRD of the NZVI-treated soil illustrated that a relative decrease in the peak intensity of clinochlore is observed in CL0+NZVI and CL9+NZVI samples. This is attributed to the pozzolanic reactions of NZVI with this mineral, leading to the destruction of its structure. On the other hand, an increase in iron compounds can be seen in the graphs because of the mixing of the samples with NZVI.

### *Field emission scanning electron microscopy (FESEM)*

The field emission scanning electron microscopy (FESEM) was used to study the fabric of the clean, contaminated, and treated specimens with NZVI.

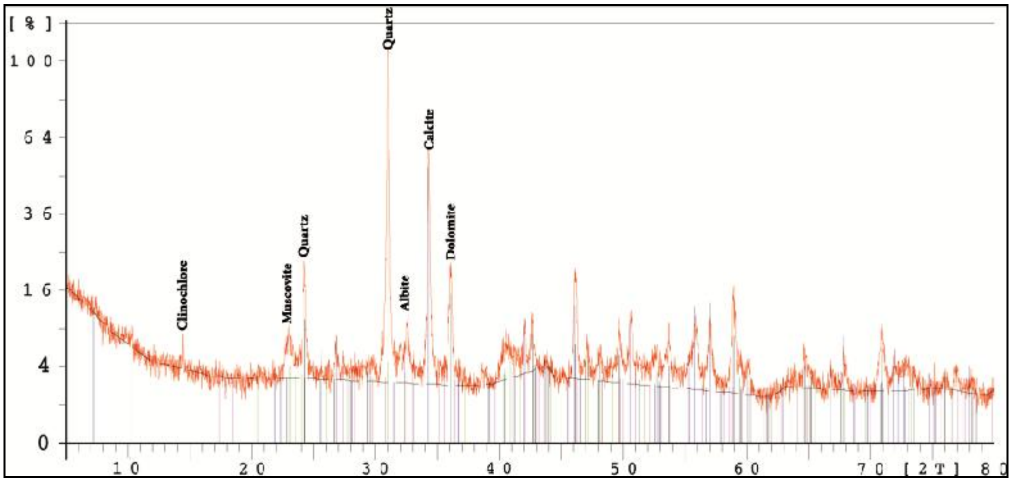

Figure 3. XRD results for natural clean clay

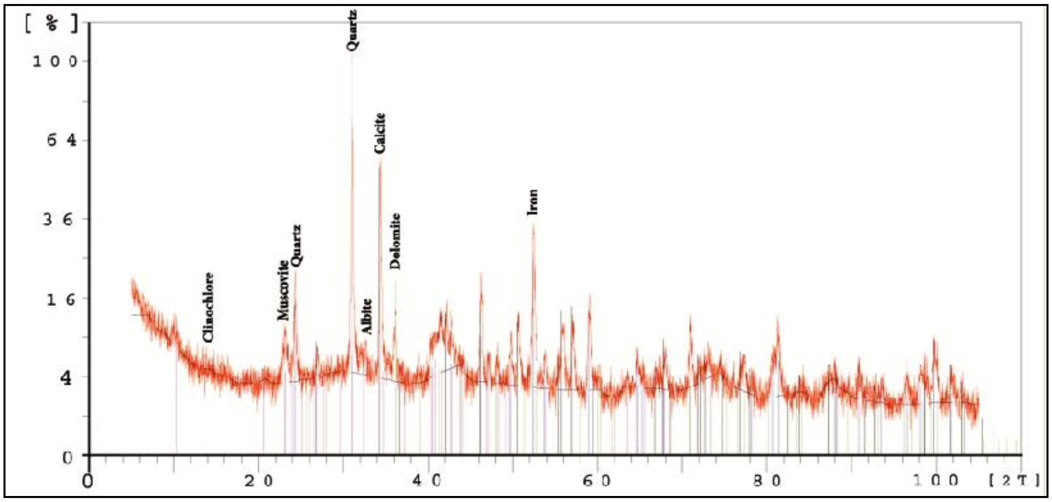

Figure 4. XRD results for CL0+NZVI sample

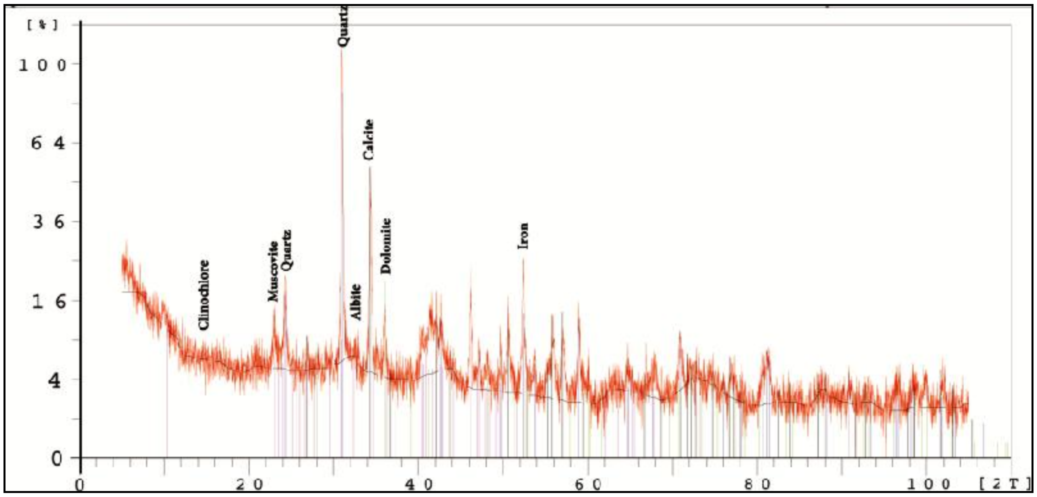

Figure 5. XRD results for CL9+NZVI sample

The fabric of a soil refers to the geometric arrangement of the soil particles. It is an important parameter controlling the engineering behavior of soils. Two types of fabric, dispersed and flocculated, exist among clay mineral particles.

In the case of net repulsion, the particles tend to assume a face-to-face orientation. This is referred to as a dispersed fabric. If, on the other hand, there is net attraction, the orientation of the particles tends to be edge-to-face or edge-to-edge. This is referred to as a flocculated fabric. In natural clays which normally contain a significant proportion of large, bulky particles, the structural arrangement can be extremely complex (Craig, 1990).

Optical microscopy of the clay sample by Olgun and Yildiz (2010) indicated that the clay particles coagulated forming an aggregate structure in the presence of the organic fluids with low dielectric constants. When the pore fluid was distilled water, the particles were separated. The degree of aggregation increased when the dielectric constant decreased and when the fluid/water ratio increased. Khosravi *et al*. (2013) also reported the flocculation of a clayey soil after mixing with gas oil.

Figure 6a-e shows the results of the fabric study of CL soil. In the clean soil, dispersed fabric is observed in the clay and fine particles (Fig. 6a).

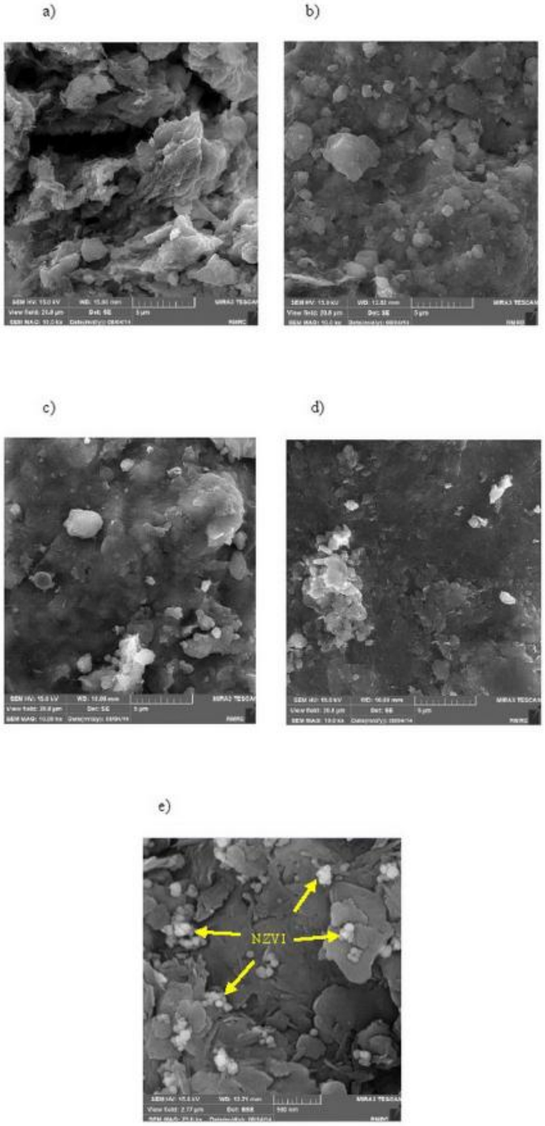

Figure 6. FESEM images; a) clean CL, b) CL + optimum moisture content, c) CL + 9% gas oil, d) CL + optimum moisture content + 9% gas oil, e) CL + optimum moisture content + 9% gas oil + 5% NZVI

A moderately dispersed fabric can be seen when the soil is mixed with optimum water content. In addition, the water surface tension has bonded the fine particles together in separated groups (Fig. 6b). The mixture of soil sample with 9% of gas oil caused a moderately flocculated fabric in the clay and fine particles (Fig. 6c). The combination effect of water and gas oil extended the flocculation in the soil specimens (Fig. 6d). It is observed that gas oil could increase the water capability to form a flocculated structure for the soil. Figure 6e shows a contaminated sample with 9% of gas oil and optimum moisture content mixed with 5% of NZVI. It can be seen that the spherical particles of NZVI sat on the surface and penetrated into the spaces between the sheets of clay particles. They did not have any significant effects on the degree of flocculation, but some of them connected the clay particles together. This is because of the attraction between the positive ζ potential of NZVI (Table 5) and the negative charges on the surface of the clay particles.

### *Effect of NZVI dosage on gas oil removal*

Zero-valent iron ($Fe^{\circ}$) has long been recognized as an excellent electron donor, regardless of its particle size (Eq. 1). This particle also readily reacts with a wide variety of redox-amenable contaminants (Zhang and Elliott, 2006). Many hydrocarbon compounds reduce due to the reaction with these particles. The role of these electron donors in the reduction of hydrocarbons has been extensively documented. For example, Matheson and Tratnyek (1994) proposed three possible mechanisms: (1) direct reduction at the metal surface, (2) reduction by ferrous iron, and (3) reduction by hydrogen with catalysis.

Apart from the surface area and particle size that were constant in this research, the NZVI dosage was also an important factor for gas oil removal. Increasing the dosage of iron particles speeds up the reaction substantially, since gas oil encounters the more surface-active sites of iron particles. Figure 7 shows gas oil removal efficiency as a function of time by various nanoscale iron dosages. As shown in the graph, the maximum removal of gas oil compounds due to the reaction with 1, 3, 5, and 7% of NZVI for CL samples was about 30, 46, 52, and 54% respectively. After 24 days, the reaction was almost stopped (Table 7). The reaction may have stopped because of two reasons: (1) NZVI is quickly oxidized to form Fe (II) and Fe (III) products (Joo *et al*., 2005; Lee *et al*., 2007). On the other hand, iron hydroxide formed on the NZVI surface because of its contact with water (Shimizu *et al*., 2012). These may decrease the electron transfer and the decomposition rate of the contaminant. (2) Reduction of hydrocarbon compounds promotes in the presence of $H^+$; therefore, the consumption of the proton and lack of it in the soil can have stopped the reaction. Figure 7 also shows the optimum percentage of NZVI and time to reach the maximum removal of gas oil, which are 5% and 24 days, respectively.

### *Effect of NZVI on the pH of the soil*

Table 7 and Figure 8 show the pH variation of the soil samples. The pH of clean soil was 6.69. After mixing samples with 9% of gas oil and optimum water content, a very low increment of pH has been seen in the soil. The pH of clean and contaminated specimens mixed with optimum moisture content and 5% of nanoscale zero-valent iron (CL0+NZVI and CL9+NZVI) increased with time; however, after 17 to 24 days, it has been almost fixed.

NZVI can form redox couples with many environmentally significant and redox-amenable electron acceptors, including hydrogen ions, dissolved oxygen (DO), nitrate, and sulfate (Matheson and Tratnyek, 1994). For example, under aerobic conditions, NZVI can react with DO as follows:

$$2Fe^{\circ} + 4H^+ + O_2 \longrightarrow 2Fe^{2+} + 2H_2O \qquad (5)$$

Implicit in the above stoichiometry is the transfer of four electrons from the iron surface and the associated increase of pH (based on the consumption of protons). The increasing pH favors the formation of one or more iron hydroxide or carbonate-based precipitates, which can have the effect of lessening reactivity at the metal surface (Matheson and Tratnyek, 1994). In anaerobic or low DO environments, NZVI also forms an effective redox couple with water as follows (Zhang and Elliott, 2006):

$$Fe^{\circ} + 2H_2O \longrightarrow 2Fe^{2+} + H_2 + 2OH^- \qquad (6)$$

This reaction also increases the pH of the environment due to the production of $OH^-$. As mentioned previously, the reduction of hydrocarbon compounds associated with proton ($H^+$) consumption can increase the pH of the environment.

*Atterberg limits*

Atterberg limits are extensively used for identification, description, and classification of cohesive soils and as a basis for the preliminary assessment of their mechanical properties. The limits consist of liquid limit (LL), plastic limit (PL) and shrinkage limit (SL). Liquid and plastic limits controlled the consistency of fine-grained soils.

The results indicated that the liquid limit (LL) and the plastic limit (PL) of the untreated soil increased with increasing the contaminant percent (Fig. 9). The increase can be explained by the theory of the diffuse double-layer. Water molecules are polar. As a result, a water molecule has a positive charge at one side and a negative charge at the other.

Table 7. The variations of gas oil removal percent and pH of the samples with time

| Sample Name | Elapsed Time (Days) | Gas oil Removal (%) | pH |
|---|---|---|---|
| **CL9** | 3 | 1.01 | 6.73 |
| | 10 | 2.34 | 6.77 |
| | 17 | 3.09 | 6.78 |
| | 24 | 4.51 | 6.79 |
| | 31 | 5.29 | 6.77 |
| | 38 | 5.51 | 6.75 |
| **CL9+1%NZVI** | 3 | 5.11 | – |
| | 10 | 10.15 | |
| | 17 | 18.11 | |
| | 24 | 29.58 | |
| | 31 | 31.35 | |
| | 38 | 31.29 | |
| **CL9+3%NZVI** | 3 | 6.22 | – |
| | 10 | 13.53 | |
| | 17 | 26.72 | |
| | 24 | 44.04 | |
| | 31 | 45.34 | |
| | 38 | 45.00 | |
| **CL9+5%NZVI (CL9+NZVI)** | 3 | 12.51 | 7.26 |
| | 10 | 21.36 | 7.43 |
| | 17 | 39.18 | 7.59 |
| | 24 | 51.29 | 7.63 |
| | 31 | 52.07 | 7.62 |
| | 38 | 53.12 | 7.64 |
| **CL9+7%NZVI** | 3 | 11.28 | – |
| | 10 | 26.73 | |
| | 17 | 42.01 | |
| | 24 | 52.76 | |
| | 31 | 53.91 | |
| | 38 | 54.01 | |
| **CL0+NZVI (CL0+5%NZVI)** | 3 | – | 7.24 |
| | 10 | | 7.31 |
| | 17 | | 7.40 |
| | 24 | | 7.42 |
| | 31 | | 7.45 |
| | 38 | | 7.43 |

It is known as a dipole. Dipole water is attracted both by the negatively charged surface of the clay particles and by the cations in the double layer. The other mechanism by which water is attracted to clay particles is hydrogen bonding, where hydrogen atoms in the water molecules are shared with oxygen atoms on the surface of the clay. All of the water held to clay particles by force of the attraction is known as double-layer water. The innermost layer of the double-layer water that is held very strongly by the clay is known as adsorbed water.

This orientation of water around the clay particles gives fine-grained soils their plastic properties. The water in the pore space that is not absorbed by the clay particles and moves easily in the soils is called free water. The free water determines the liquid behavior of the soil (Das, 1994). Unlike the water molecule, the gas oil molecule is not diploe.

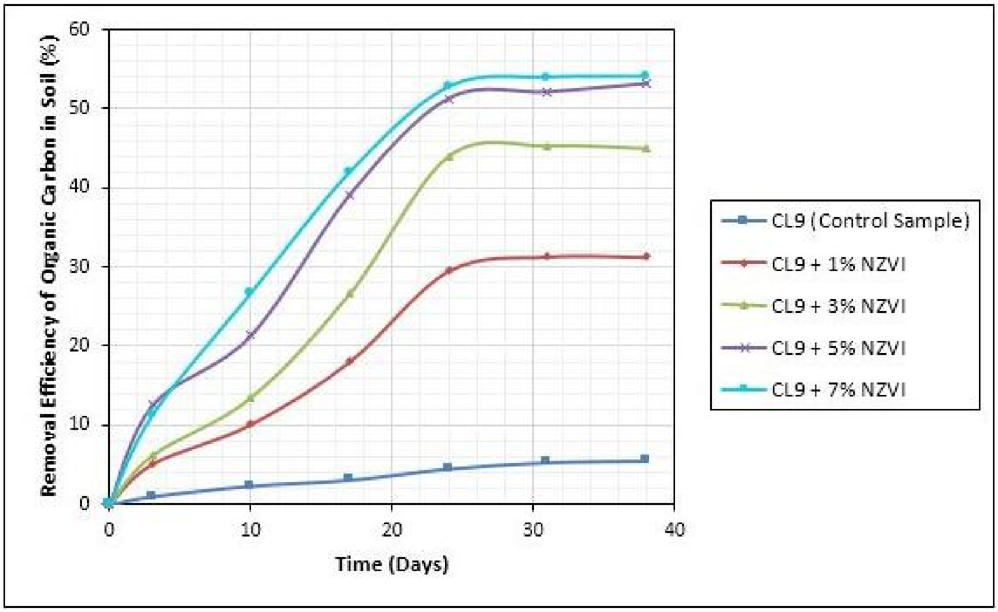

Figure 7. Gas oil removal efficiency vs. time for different percent of NZVI

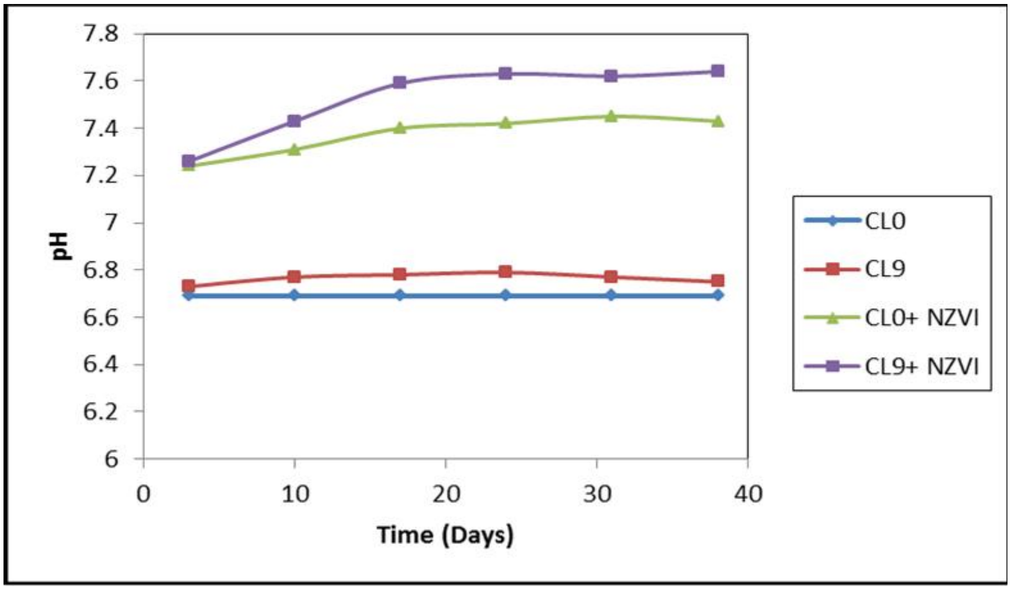

Figure 8. pH variations of the clean, contaminated and treated soil samples

Therefore, as the gas oil is mixed with soil, it covers the soil particles and does not allow water molecules to develop the double-layer, so more water is needed for the soil to obtain plastic properties. This might be the reason for the increase in the plastic limit. However, if the oil orients the soil particles, most of the water added to the soil during the test will join the free water, so the liquid limit shows a slight increase with the increasing gas oil content (Kermani & Ebadi, 2012). With the increase of the liquid and plastic limit, the plasticity index (PI) of the soil specimens decrease.

The LL and PL of the treated soil (with 5% of NZVI and after 24 days) decreased in all the contents of gas oil contamination (Table 8 and Fig. 9). The following reasons could explain this behavior: (1) NZVI powder is inherently non-plastic; therefore, adding the powder to the soil causes a decrease in the plastic property of the treated soil specimens. (2) Decomposition of more than 50% of gas oil due to the reaction with NZVI decreased the content of the contaminant in the soil, which increased the Atterberg limits before. With the decrease of LL and PL, the plasticity index (PI) of the soil decreased. In general, soil with smaller PI has better workability in engineering practice.

### *Compaction tests*

The results of compaction test are plotted in Figures 10 and 11. In the first stage, compaction test was carried out on the soil samples with 0, 3, 6, and 9% of gas oil. The curves of the contaminated specimens are generally located to the left side of the uncontaminated soils. They generally show a reduction in maximum dry density with the increase of gas oil content. In all of the contaminated samples, the presence of oil reduces the amount of water needed to reach maximum dry density (Fig. 11). This describes the lubricating effect of gas oil that alters the soil to a state of looser material than uncontaminated soil (Rahman *et al*., 2010).

Table 8. The results of geotechnical tests

| **Sample Name** | **LL (%)** | **PL (%)** | **PI (%)** | **$w_{opt}$ (%)** | **$\rho_{dmax}$ (g/cm$^3$)** | **C (KN/m$^2$)** | **φ (Degree)** |
|---|---|---|---|---|---|---|---|
| **CL0** | 47.87 | 23.45 | 24.42 | 21.2 | 1.61 | 12.13 | 18.56 |
| **CL3** | 55.34 | 29.23 | 26.11 | 20.9 | 1.49 | 11.38 | 13.58 |
| **CL6** | 58.76 | 33.73 | 25.03 | 20.0 | 1.48 | 14.31 | 6.02 |
| **CL9** | 57.79 | 33.31 | 24.48 | 17.9 | 1.47 | 14.68 | 6.14 |
| **CL0+NZVI** | 47.14 | 21.51 | 25.63 | 21.9 | 1.73 | 58.74 | 47.48 |
| **CL3+NZVI** | 52.18 | 28.25 | 23.93 | 22.0 | 1.62 | 53.83 | 37.61 |
| **CL6+NZVI** | 54.90 | 32.38 | 22.52 | 21.3 | 1.59 | 48.80 | 28.51 |
| **CL9+NZVI** | 55.81 | 32.64 | 23.17 | 18.75 | 1.55 | 44.06 | 22.13 |

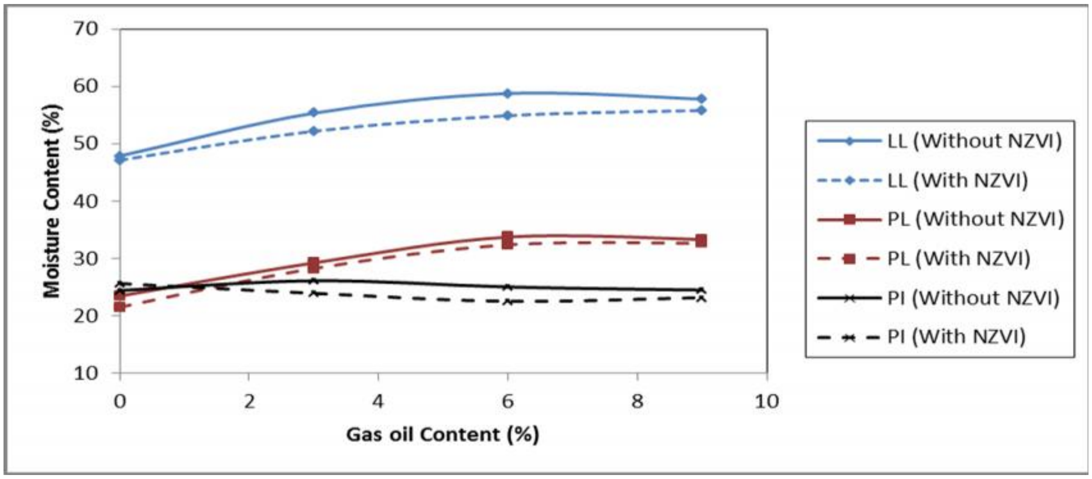

Figure 9. Variations of LL and PL for contaminated and treated soil samples

However, the results are in agreement with those reported by Khamechiyan *et al*. (2007), but inconsistent with the findings of Al-sanad *et al*. (1995) and Meegoda *et al*. (1998). Their researches show an increase in maximum dry density with increasing oil contamination up to about 4% and then reduction in maximum dry density with increasing oil content.

In the second stage, compaction test was performed to determine the effect of NZVI on maximum dry density and optimum water content. After mixing of the contaminated soil samples with 5% of NZVI and at the end of the curing time (24 days), the results show that the maximum dry density and optimum water content of all the treated samples increased (Table 8). The following reasons could explain this behavior: (1) The specific gravity of NZVI (Table 5) is higher than the specific gravity of the soil (Table 1).

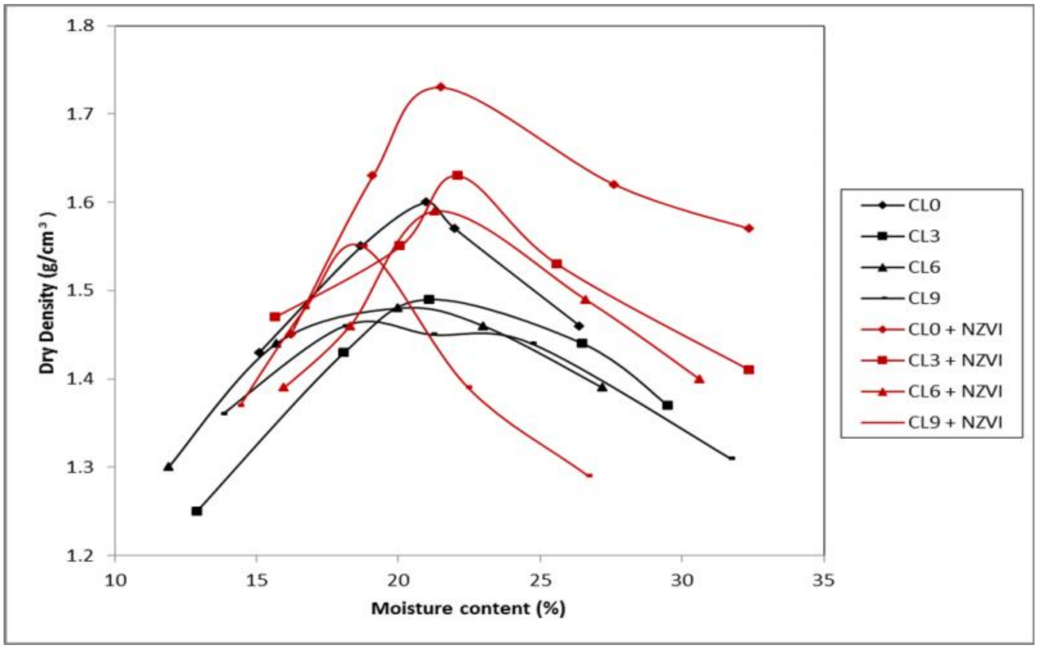

Figure 10. Compaction curves for the clean, contaminated and treated soil samples

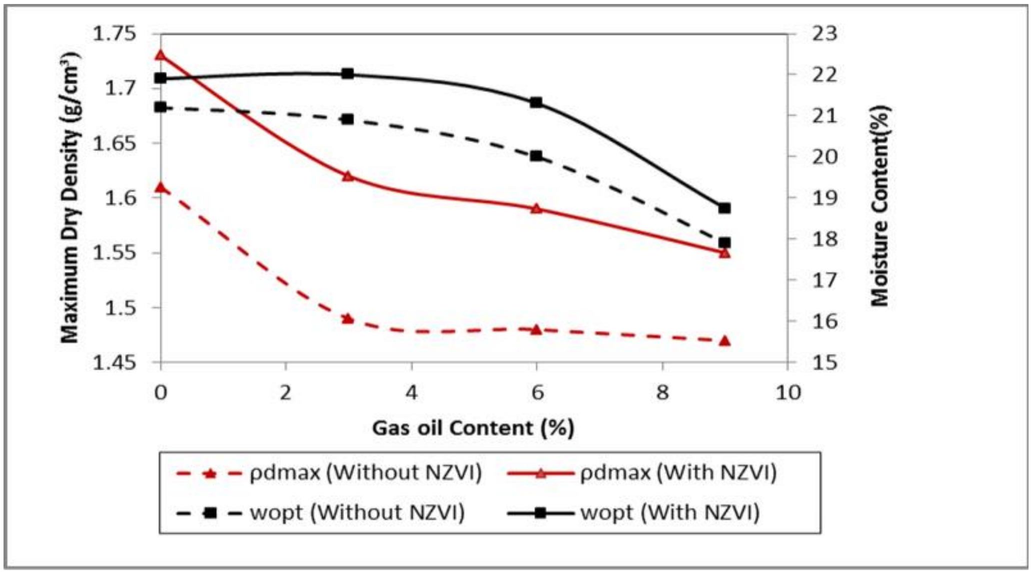

Figure 11. Maximum dry density and optimum moisture content variations of the clean, contaminated and treated soil samples

(2) The pozzolanic reaction between the clay present in the soil and NZVI was responsible for the increase in optimum moisture content. (3) Transformation of more than 50% of gas oil composition owing to the reaction with NZVI reduced the percentage of contaminant in the soil, which decreased the optimum moisture content before.

*Direct shear tests*

In the first stage, direct shear tests were carried out on the clean and contaminated samples of the soil, according to ASTM D3080 (1999). The tests were performed in a square shear box (6 cm × 6 cm) with a rate of shear deformation equal to 0.5 mm/min at normal loads of 24, 44 and 64 KN/m². Figure 12 shows the relationship between the shear stress and the normal stress of the samples. The results generally indicate an increase in cohesion and a decrease in the friction angle of contaminated samples with the increase of contamination content (Figs. 13 and 14). The results are in agreement with those reported by Khosravi *et al*. (2013), but inconsistent with those found by Shah *et al*. (2003) and Kermani and Ebadi (2012). The increase in cohesion is attributed to the low dielectric constant of hydrocarbon fluids such as gas oil. According to Lambe (1958) and Sridharan and Rao (1979), the cohesion of clays increases with reduction in the dielectric constant of the pore fluid. In addition, Zhao (1996) showed that the organic materials and hydrocarbons reduce the repulsive forces between clay particles, resulting in higher cohesion. On the other hand, gas oil viscosity is more than water viscosity (Table 3). Therefore, the ability of gas oil to withstand the shear force is more than water. When shear force is applied to the specimen, in addition to soil particles, gas oil resists shear force and the apparent cohesion of the soil increases. The decrease in the friction angle in the presence of gas oil might be associated with the lubrication effect of gas oil on the surface of the particles.

In the second stage, to realize the effect of NZVI on the shear strength parameters of contaminated soil, the samples mixed with 5% of NZVI were compacted in the mold with static compaction at the determined maximum dry density and optimum moisture content.

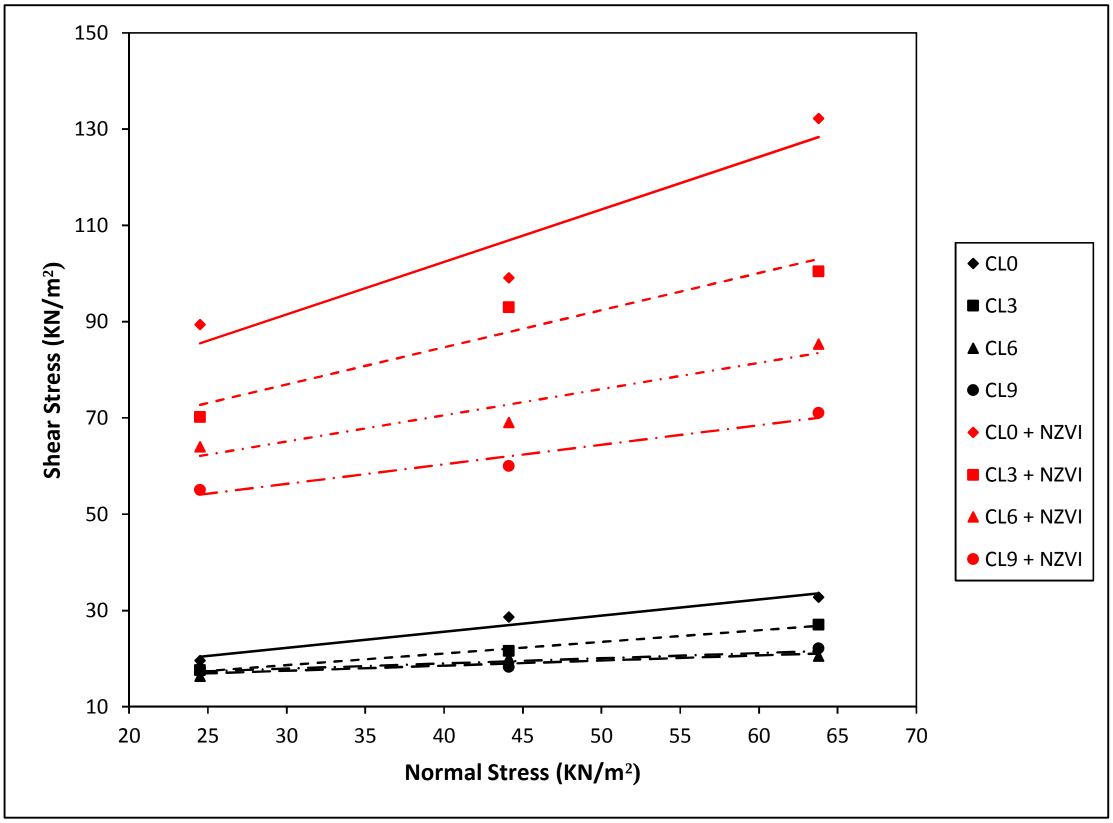

Figure 12. Relationship between shear stress-normal stress of the untreated and treated soil samples

Then, they were covered with a plastic cover and direct shear tests were carried out on them after 24 days (Fig. 15). The results showed a great significant increase in cohesion (C) and internal friction angle (φ) of the treated soil (Table 8, Figs. 13 and 14). The following statements could explain this behavior: (1) it has been well established that the pH of the environment strongly influences the ζ potential of the particles. Specifically, as the pH increases, the particles tend to acquire additional negative charge, which translates into more negative ζ potential (Zhang and Elliott, 2006). The NZVI used in this study had a ζ potential equal to +17.4 in neutral pH (Table 5). Figure 8 shows that the pH of clean, contaminated, and treated samples change from 6.7 to 7.6; therefore, it is expected that the ζ potential of NZVI remain positive during the study. On the other hand, the surface of clay mineral particles carry residual negative charges, mainly as a result of the isomorphous substitution of aluminum or silicon atoms by atoms of lower valency, but also due to the disassociation of hydroxyl ions (Craig, 1990; Das, 1994). Therefore, the attraction force between the NZVI and surface of clay particles could be a reason for the increase of cohesion (C) in the clean sample.

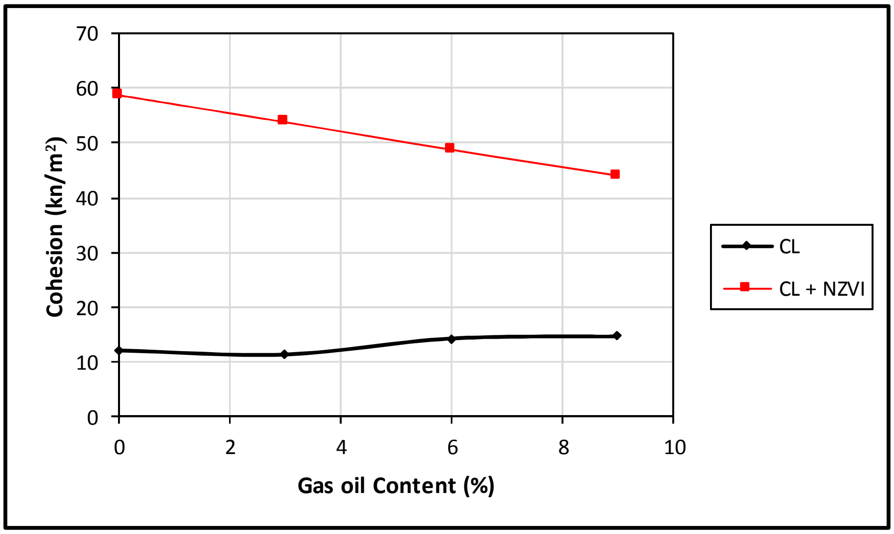

Figure 13.Variations of cohesion in the untreated and treated soil samples

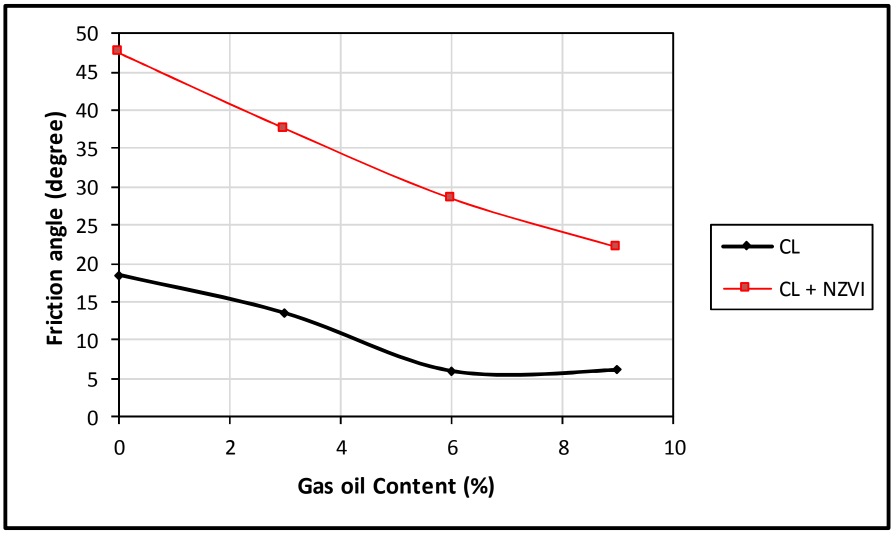

Figure 14.Variations of internal friction angle in the untreated and treated soil samples

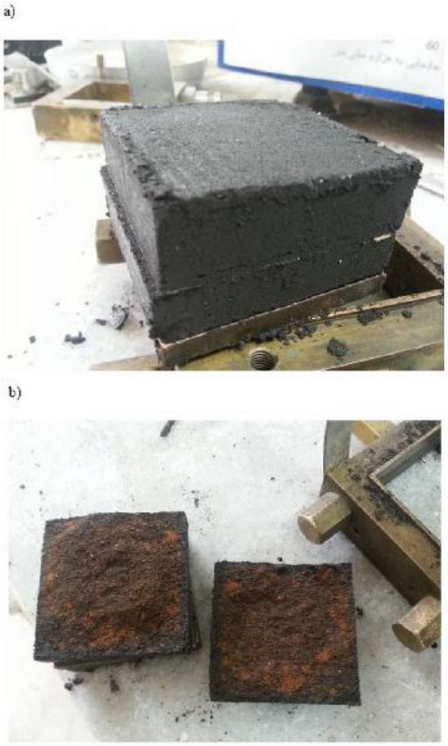

Figure 15. Direct shear test; a) a treated sample by NZVI at the end of the test, b) transformation of $Fe^{o}$ to $Fe^{2}+$ (orange spots) due to the mentioned reactions

This attractive force decreased with increasing of gas oil content because a film of contaminant covered the surface of the clay mineral. (2) The presence of residual gas oil in the soil increases the cohesion due to the reasons that were mentioned before. (3) Decreasing of gas oil contamination due to its reaction with NZVI, as previously mentioned, is another reason for the increase of cohesion (C) and internal friction angle (φ). (4) NZVI powder is inherently a non-plastic and frictional matter; therefore, adding the powder to the soil samples causes an increase in the internal friction angle.

## Conclusions

Zero-valent iron (ZVI) has found usage in the remediation of water, soils, and sediments for removing contaminants, especially hydrocarbon compounds. Common environmental hydrocarbon contaminants such as polychlorinated biphenyls (PBCs), trichloroethene (TCE), polycyclic aromatic hydrocarbons (PAHs), etc. can be transformed by ZVI and NZVI. Nevertheless, there is no specific study on the improvement of the geotechnical properties of contaminated soils with hydrocarbon compounds, such as gas oil by NZVI. Therefore, an experimental study was performed to determine the effects of NZVI on the geotechnical characteristics of a clayey soil contaminated by gas oil. The program included Atterberg limits (LL and PL), compaction, and direct shear tests that were carried out on the clean, contaminated and treated soil specimens. The results indicated that LL and PL increased in the soil treated by NZVI, which had decreased due to the gas oil contamination before. NZVI powder is inherently non-plastic, so adding it to the soil specimens causes a decrease in the plasticity of the treated soil. The study ascertained that the maximum dry density and optimum water content of the treated soil increased because of the massive specific gravity of NZVI and the pozzolanic reaction between clay particles and NZVI, respectively. The cohesion and internal friction angle of the treated samples showed a great increase due to the decomposition of gas oil and the attractive force between NZVI and the surface of clay particles.

## References

Al-Sanad, H.A., Eid, W.K., Ismael, N.F., 1995. Geotechnical properties of oil-contaminated Kuwaiti sand. Journal of Geotechnical Engineering, 121: 407–412.

ASTM (American Society for Testing and Materials), 1999. Annual book of ASTM standards. Section 4, Construction, Soil and Rock, volume 4.08, ASTM, Philadelphia, PA.

Bhatt, I., Tripathi, B.N., 2011. Interaction of engineered nanoparticles with various components of the environment and possible strategies for their assessment. Chemosphere, 82: 308-317.

Brunauer, S., Emmett, P.H., Teller, E., 1938. Adsorption of gases in multimolecular layers. Journal of the American Chemical Society, 60: 309–319.

Carter, D.L., Heilman, M.D., Gonzalez, C.L., 1965. Ethylene glycol monoethyl ether for determining surface area of silicate minerals. Soil Science, 100: 356-360.

Chang, M.C., Shu, H.Y., Hsieh, W.P., Wang, M.C., 2005. Using nanoscale zero-valent iron for the remediation of polycyclic aromatic hydrocarbons contaminated soil. Journal of the Air and Waste Management Association, 55: 1200-1207.

Craig, R.F., 1990. Soil Mechanics. 4th edition, Chapman and Hall, 410pp.

Das, B.M., 1994. Principle of Geotechnical Engineering. 3rd edition, PWS Publishing Company, 436pp.

Gillham, R.W., O'Hannesin, S.F., 1994. Enhanced degradation of halogenated aliphatics by zero-valent iron. Groundwater, 32: 958-967.

Joo, S.H., Feitz, A.J., Sedlak, D.L., Waite, T.D., 2005. Quantification of the oxidizing capacity of nanoparticulate zero-valent iron. Environmental Science and Technology, 39: 1263-1268.

Kermani, M., Ebadi, T., 2012. The effect of oil contamination on the geotechnical properties of fine-grained soils. Soil and Sediment Contamination, 21: 655–671.

Khamehchiyan, M., Charkhabi, A.H., Tajik, M., 2007. Effect of crude oil contamination on geotechnical properties of clayey and sandy soils. Engineering Geology, 89: 220–229.

Khosravi, E., Ghasemzadeh, H., Sabour, M.R., Yazdani, H., 2013. Geotechnical properties of gas oil-contaminated kaolinite. Engineering Geology, 166: 11–16.

Lambe, T.W., 1958. The engineering behavior of compacted clay. Journal of the Soil Mechanics and Foundation Division, ASCE, 84: 1–35.

Lee, J., Kim, J., Choi, W., 2007. Oxidation on zerovalent iron promoted by polyoxometalate as an electron shuttle. Environmental Science and Technology, 41: 3335-3340.

Li, A.Q., Elliott, D.W., Zhang, W.X., 2006. Zero-valent iron nanoparticles for abatement of environmental pollutants: materials and engineering aspects. Critical Reviews in Solid State and Materials Sciences, 31: 111-122.

Lien, H.L., Zhang, W.X., 1999. Dechlorination of chlorinated methanes in aqueous solution using nanoscale bimetallic particles. Journal of Environmental Engineering, 125: 1042-1047.

Matheson, L.J., Tratnyek, P.G., 1994. Reductive dehalogenation of chlorinated methanes by iron metal. Environmental Science and Technology, 28: 2045-2053.

Meegoda, J.N., Chen, B., Gunasekera, S.D., Pederson, P., 1998. Compaction characteristics of contaminated soils-reuse as a road base material. In: Vipulanandan, C., Elton, David J. (Eds.), Recycled Materials in Geotechnical Applications. Geotechnical Special Publication, ASCE, 79: 165–209.

Nowack, B., Bucheli, T.D., 2007. Occurrence, behavior and effects of nanoparticles in the environment. Environmental Pollution, 150: 5-22.

Olgun, M., Yildiz, M., 2010. Effect of organic fluids on the geotechnical behavior of a highly plastic clayey soil. Applied Clay Science, 48: 615–621.

Pierce, J.W., Siegel, F.R., 1969. Quantification in clay mineral studies of sediments and sedimentary rock. Journal of Sedimentary Petrology, 39: 187-193.

Rahman, Z.A., Hamzah, U., Taha, M.R., Ithnain, N.S., Ahmad, N., 2010. Influence of oil contamination on geotechnical properties of basaltic residual soil. American Journal of Applied Sciences, 7: 954–961.

Shah, S.J., Patel, A.V., Tiwari, K.C., Ramakrishnan, D., 2003. Stabilization of fuel oil contaminated soil - A case study. Geotechnical and Geological Engineering, 21: 415-427.

Shimizu, A., Tokumura, M., Nakajima, K., Kawase, Y., 2012. Phenol removal using zero-valent iron powder in the presence of dissolved oxygen: roles of decomposition by the fenton reaction and adsorption/precipitation. Journal of Hazardous Materials, 201: 60-67.

Song, H., Carraway, E.R., 2005. Reduction of chlorinated ethanes by nanosized zero-valent iron: kinetics, pathways, and effects of reaction conditions. Environmental Science and Technology, 39: 6237-6245.

Sridharan, A., Rao, G.V., 1979. Shear strength behavior of saturated clays and the role of the effective stress concept. Geotechnique, 29: 177–193

Tratnyek, P.G., Johnson, R.L., 2006. Nanotechnology for environmental cleanup. Nanotoday, 1: 44-48.

Varanasi, P., Fullana, A., Sidhu, S., 2007. Remediation of PCB contaminated soils using iron nano-particles. Chemosphere, 66: 1031-1038.

Wang, C.B., Zhang, W.X., 1997. Synthesizing nanoscale iron particles for rapid and complete dechlorination of TCE and PCBs. Environmental Science and Technology, 31: 2154-2156.

Zhang, W.X., 2003. Nanoscale iron particles for environmental remediation, an overview. Journal of Nanoparticle Research, 5: 323-332.

Zhang, W.X., Elliott, D.W., 2006. Application of iron nanoparticles for groundwater remediation. Remediation Journal, 16: 7-21.

Zhang, Z.Y., Lu, M., Zhang, Z.Z., Xiao, M., Zhang, M., 2012. Dechlorination of short chain chlorinated paraffins by nanoscale zero-valent iron. Journal of Hazardous Materials, 243: 105-111.

Zhao, D., 1996. Experimental study of stress-strain and shear strength behavior of contaminated cohesive soils. Ph.D. thesis, Whiting School of Engineering, The Johns Hopkins University.